



<b>Title</b>	Investigating the Effect of Persistent Inward Currents on Motor Unit Firing Rates and Beta-Band Coherence in a Model of the First Dorsal Interosseous Muscle
<b>Authors(s)</b>	Senneff, Sageanne, McManus, Lara M., Lowery, Madeleine M.
<b>Publication date</b>	2019-07-27
<b>Publication information</b>	Senneff, Sageanne, Lara M. McManus, and Madeleine M. Lowery. "Investigating the Effect of Persistent Inward Currents on Motor Unit Firing Rates and Beta-Band Coherence in a Model of the First Dorsal Interosseous Muscle." IEEE, July 27, 2019. <a href="https://doi.org/10.1109/embc.2019.8857534">https://doi.org/10.1109/embc.2019.8857534</a> .
<b>Conference details</b>	The 41st Annual International Conference of the IEEE Engineering in Medicine and Biology Society (EMBC), Berlin, Germany, 23-27 July 2019
<b>Publisher</b>	IEEE
<b>Item record/more information</b>	<a href="http://hdl.handle.net/10197/11279">http://hdl.handle.net/10197/11279</a>
<b>Publisher's statement</b>	© 2019 IEEE. Personal use of this material is permitted. Permission from IEEE must be obtained for all other uses, in any current or future media, including reprinting/republishing this material for advertising or promotional purposes, creating new collective works, for resale or redistribution to servers or lists, or reuse of any copyrighted component of this work in other works.
<b>Publisher's version (DOI)</b>	10.1109/embc.2019.8857534

Downloaded 2026-05-01 23:36:45

The UCD community has made this article openly available. Please share how this access benefits you. Your story matters! (@ucd\_oa)



© Some rights reserved. For more information

1 **Investigating the Effect of Persistent Inward Currents on Motor Unit**  
2 **Firing Rates and Beta-Band Coherence in a Model of the First Dorsal**  
3 **Interosseous Muscle**

4 Author List: Sageanne Senneff, Lara McManus and Madeleine M. Lowery

5 Corresponding Author: Dr Madeleine Lowery

6 School of Electrical and Electronic Engineering,

7 University College Dublin, Belfield, Dublin 4, Ireland

8 madeleine.lowery@ucd.ie

9 **Affiliations:** S Senneff, L McManus and M. M. Lowery are with the School of Electrical and  
10 Electronic Engineering, University College Dublin, Ireland. (e-mail:  
11 sageanne.senneff@ucdconnect.ie, madeleine.lowery@ucd.ie).

12 **Link to Published Manuscript, DOI:** 10.1109/EMBC.2019.8857534

13 **Details of Funding:** Research supported by the European Research Council: ERC-2014-CoG-  
14 646923\_DBSSModel.

15 © 2019 IEEE. Personal use of this material is permitted. Permission from IEEE must be  
16 obtained for all other uses, in any current or future media, including reprinting/republishing this  
17 material for advertising or promotional purposes, creating new collective works, for resale or  
18 redistribution to servers or lists, or reuse of any copyrighted component of this work in other  
19 works.

## 20 **Abstract**

21 Neuromodulatory drive resulting in the generation of persistent inward currents (PICs) within  
22 motoneuron dendrites has been demonstrated to introduce nonlinearities into the motoneuron  
23 input-output function for a given motor command. It is less understood, however, as to what  
24 role PICs play during voluntary contractions or on the correlation between motoneuron firings  
25 arising as a result of common synaptic inputs to the motoneuron pool. To examine this, a  
26 biophysical model of the motoneuron pool representing the first dorsal interosseous (FDI)  
27 muscle was used to simulate the effects of PICs on motor unit firing patterns and beta-band (15-  
28 30 Hz) motor unit coherence at 20, 30, and 40 percent of maximum voluntary contraction  
29 (MVC). The contribution of PICs at each MVC was quantified by calculating the difference in  
30 the mean firing rate of each motoneuron within the pool and assessing changes in the mean  
31 firing rate distribution and motor unit coherence with and without PICs present. The results of  
32 the current study demonstrated that increased activation of PICs progressively reduced motor  
33 unit coherence, however, changes in coherence were modest when investigating activation  
34 levels consistent with experimentally observed mean motor unit firing rates in the FDI muscle  
35 during isometric voluntary contraction.

## 36 **Introduction**

37 Motoneurons within the spinal cord are tasked with integrating thousands of excitatory,  
38 inhibitory, and neuromodulatory synaptic inputs and translating them into motor unit action  
39 potentials, triggering muscle activation. It is well established that motor unit firing patterns are  
40 strongly influenced by neuromodulatory drive, known to induce nonlinearities in synaptic  
41 integration by exciting voltage-dependent, dendritic ion channels that produce persistent inward  
42 currents (PICs) [1-6]. Recent studies have further hypothesized that the level of  
43 neuromodulatory drive sets the excitability of the motoneuron pool across all motor tasks,  
44 including highprecision movements, acting as the gain of the motoneuron input-output function  
45 [4-6]. Pre-synaptic branched inputs and descending oscillatory inputs, widely believed to be of  
46 cortical origin, are two major sources of common input to the motoneuron pool, leading to  
47 synchronization between motor unit firing times and increased coherence in the beta-band (15-  
48 30 Hz) region [7-9]. Motor unit synchronization has been observed in the first dorsal  
49 interosseous (FDI) muscle during sustained voluntary isometric contractions, and has been  
50 demonstrated to be greater in the non-dominant versus the dominant hand [10-11]. A recent  
51 study showed, for the first time, that betaband motor unit coherence in the FDI muscle increases  
52 during fatiguing contractions and post-fatigue, compared to pre-fatigue estimates [9]. Open  
53 questions remain as to what effect PICs have on motor unit firing patterns and beta-band motor

54 unit coherence in the presence of common cortical inputs. An experimental study in turtle  
55 motoneurons demonstrated that the recruitment of PICs led to reduced motor unit  
56 synchronization [12], however it was recently demonstrated that PIC-induced motoneuron  
57 depolarization is smaller in larger animals, and therefore may play a smaller role during  
58 voluntary contraction in humans [13]. Previous computational studies assessing changes in  
59 intramuscular and corticomuscular coherence found contrasting results when looking at the  
60 effect of PICs on either branched or oscillatory common inputs, however this was attributed to  
61 the difference in methodological approaches when introducing common or correlated synaptic  
62 inputs [8,14]. To examine this issue in the present study, a biophysical model of the motoneuron  
63 pool was developed for the FDI muscle that was driven by physiological, cortical spike trains  
64 generated for a range of force levels. The model was used to investigate the contribution of PICs  
65 on motor unit firing rates for increasing levels of maximum voluntary contraction (MVC), as  
66 well as changes in the beta-band coherence spectra in response to increased recruitment of PIC-  
67 generating ion channels within motoneuron dendrites.

## 68 **Methods**

69 A biophysical model of the motoneuron pool representing the first dorsal interosseous (FDI)  
70 muscle was implemented in NEURON [15] and used to investigate the effect of PICs on beta-  
71 band motor unit coherence in response to correlated synaptic inputs for simulated voluntary  
72 contractions across a range of force levels. The model was developed from a model developed  
73 previously for cat MG and human tibialis anterior motoneurons [6], and adapted for the FDI  
74 muscle.

### 75 *A. Model Structure*

76 Each of the 100 motoneurons within the pool were modelled with a five-compartment structure  
77 that included a single soma and four dendritic branches. A persistent sodium channel was placed  
78 within the soma, as well as four other ionic channels: a transient sodium channel, a  
79 delayedrectifier potassium channel, a calcium-dependent potassium channel, and a  
80 Hyperpolarization-activated cyclic nucleotiddegated (HCN) channel [6]. A slowly inactivating,  
81 voltage-dependent persistent calcium channel was placed within each dendrite, and the maximal  
82 conductance for each dendrite was varied to ensure unique plateau generation across the four  
83 branches [6]. To adapt this model for the FDI, the maximal conductances of the calcium  
84 channels were proportionally reduced across the dendrites, uniformly for each motoneuron  
85 within the pool, in order to generate plateau potentials resulting in mean motor unit firing rates  
86 within the range reported experimentally for the FDI [16-17].

### 87 *B. Synaptic Inputs*

88 A synaptic input was introduced to each motoneuron, at each dendrite, containing three  
89 components: an independent excitatory signal, an independent inhibitory signal, and a beta-  
90 modulated common signal. The relative contribution of the inhibitory component to the overall  
91 independent input (i.e. excitatory + inhibitory) was 25%, while the relative contribution of the  
92 common component to the overall synaptic input (i.e. independent + common) was 44%. The  
93 ratio of common to independent input was chosen based upon experimental findings in wrist  
94 extensor muscles, and adjusted to generate motor unit coherence spectra qualitatively similar to  
95 experimental recordings in the FDI [9, 18]. To generate the common signal, a random Gaussian  
96 noise signal was band-pass filtered between 12-22 Hz and introduced into an integrate and fire  
97 model to generate 2000 weakly beta-modulated cortical spike trains [19]. Each motoneuron  
98 received the summation of 100 randomly chosen spike trains, such that 5% of the common input  
99 was shared between each motoneuron, combining the effects of presynaptic branching and  
100 common oscillatory modulation. A single compartment motoneuron pool model was used to

101 determine the synaptic inputs required to drive the motor unit firing at rates that produce a target  
102 force of 20%, 30% and 40% of maximum voluntary contraction (MVC) [20]. The resulting  
103 signals were then used as inputs to the biophysical motoneuron pool model described in the  
104 current study.

### 105 **C. Data Analysis**

106 To estimate the contribution of PICs on motor unit firing rates at a range of low-force to high-  
107 force voluntary contractions, the model was first fit to the available experimental data in the FDI  
108 muscle with PICs intact on the dendrites. PICs were then removed from the model at each force  
109 level, and the  $\Delta F$  value was calculated as the changing in firing rate after PIC removal for each  
110 motoneuron within the pool. To approximate the effect of PICs on the beta-band motor unit  
111 coherence spectra, firing times were extracted for each motoneuron within the pool during  
112 simulations performed with increasing dendritic calcium channel densities: 0.0, 1.0, 1.25, 1.50,  
113 and 1.75. To control for changes in mean firing rate at each force level in the presence of  
114 increasing activation of PICs, each component of the synaptic input was reduced proportionally  
115 to maintain the same ratio of excitatory, inhibitory, and common input. A subset of 26  
116 motoneurons, with a cut-off firing frequency of 7 Hz, was chosen at random for coherence  
117 analysis at each force level. The subset was split into two groups for coherence analysis using  
118 the composite spike train method [10], such that coherence was calculated for all possible  
119 combinations of motoneurons within the subset. The same subset was used to calculate  
120 coherence at all force levels, for each calcium channel density.

## 121 **Results**

122 The mean firing rate distribution for the FDI model across force levels is presented in Figures  
123 1A-1C. In order to visualize the contribution of PICs at each MVC, the resulting mean firing  
124 rate distribution after removing PICs in the model is presented in shaded gray. The mean firing  
125 rate across all recruited motoneurons within the pool (i.e. firing above 7 Hz) dropped from 17.6  
126 Hz to 16.1 Hz, 20.1 Hz to 18.0 Hz, and 22.5 Hz to 19.7 Hz at 20%, 30%, and 40% MVC,  
127 respectively, when removing PICs from the model. The mean firing rate range was broader  
128 when PICs were included in the model, presenting as 20.0 Hz, 22.8 Hz, and 30.0 Hz at 20%,  
129 30%, and 40% MVC. When PICs were removed from the model, the mean firing rate range  
130 dropped to 15.3 Hz, 20.0 Hz, and 22.5 Hz, respectively. The whole pool mean firing rate and  
131 firing rate range is presented visually in Figure 2B for each force level, with and without the  
132 presence of PICs. In Figure 2A, the change in mean firing rate is presented individually for each  
133 motoneuron within the pool, ranging from the lowest to the highest threshold motoneuron. The

134 change in mean firing rate is represented with the value, calculated as the drop in mean firing  
135 rate when PICs were removed in the model. The average values across the recruited  
136 motoneurons within the pool were calculated as 1.9 Hz, 2.2 Hz, and 3.0 Hz for 77 motoneurons  
137 at 20% MVC, 84 motoneurons at 30% MVC, and 87 motoneurons at 40% MVC, respectively.  
138 The firing rate range presented at 5.7 Hz, 4.1 Hz, and 8.4 Hz at 20% MVC, 30% MVC, and  
139 40% MVC, with peak values of 6.7 Hz, 5.2 Hz, and 9.1 Hz at each respective force level.  
140 Plateau potentials produced by PICs within each dendrite were averaged and presented in  
141 Figures 3A-3D for the lowest-threshold motoneuron in the pool, at each force level. The PIC  
142 plateau amplitude and rate of onset increased with increasing force, a relationship that was  
143 maintained when assessing variations in calcium channel density. When increasing the density  
144 of PICs on the dendrites, the sharpest change in plateau amplitude was observed at 20% MVC,  
145 while increases were more gradual, with a higher standard deviation, for increasing force levels.  
146 The coherence spectra was calculated for each density level and presented in Figures 3E-3H. To  
147 assess the change in coherence when PICs were removed from the model (i.e. 0.0 in Figures  
148 3A-3F), whole pool mean firing rate was controlled for by adjusting the amplitude of the total  
149 synaptic input, while keeping the ratio between the common and independent components  
150 constant. The relative change in the amplitude of the synaptic input was 108.9% for both 20%  
151 and 30% MVC and 111.1 % for 40% MVC. The corresponding change in the coherence integral  
152 taken across the beta-band frequency spectrum was 119.3%, 115.5%, and 104.8%, respectively,  
153 demonstrating that PIC removal had the largest affect on coherence at 20% MVC. To assess  
154 whether increased activation of PICs affected the coherence spectra, the density of calcium  
155 channels on the dendrites was increased to 1.25, 1.5, and 1.75 times the level used to fit to  
156 experimental data in the FDI muscle. The peaks in the coherence spectra over the beta-band  
157 region were observed to decrease for increasing density levels, with the largest reduction in the  
158 coherence peaks observed at density 1.75. This reduction corresponded to a decrease in the  
159 integral of the coherence taken over the beta-band, which was reduced to 29.0%, 45.8%, and  
160 50.1% of its original value at 20%, 30%, and 40% MVC, respectively. To control for mean  
161 firing rate at this density, the total synaptic amplitude was reduced to 15.6% of its original value  
162 at 20% MVC, 26.7% of its original value at 30% MVC, and 28.9% of its original value at 40%  
163 MVC. Changes in the coherence spectra were more modest at the lower density levels, with  
164 reductions between 0-20% in the coherence integral for densities 1.25 and 1.5.

165

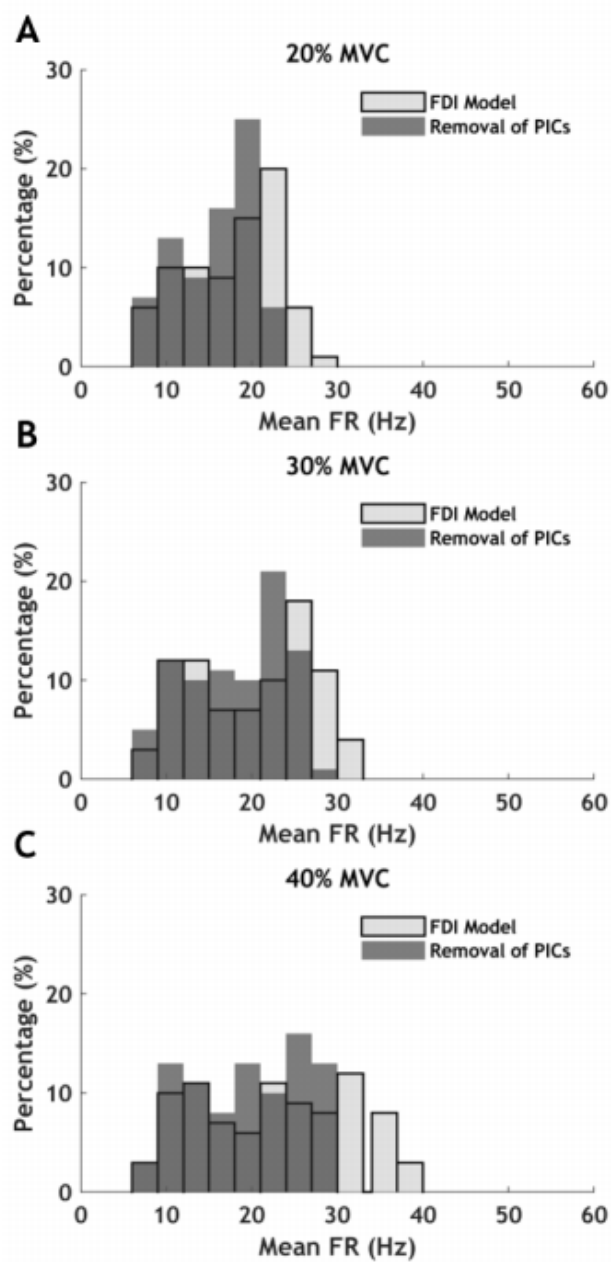
166 **Discussion;** Motor unit synchronization and increased coherence in the beta-band region has  
167 been observed during sustained, voluntary isometric contractions in the FDI muscle of the hand.  
168 Increasing evidence has suggested that PICs contribute to motor unit firing patterns across a  
169 range of motor tasks, however it is less understood as to what effect they have on branched or  
170 oscillatory common cortical inputs responsible for changes in motor unit synchronization. In  
171 order to estimate the effects of PICs on motor unit firing times and coherence in the presence of  
172 correlated synaptic inputs, a biophysical model of the motoneuron pool was developed for the  
173 FDI muscle and simulated at a range of force levels. To the best of our knowledge, there has yet  
174 to be an experimental study to quantify the contribution of PICs on motor unit firing rates in the  
175 FDI, however studies in the human upper and lower limb have found that PICs can increase  
176 motor unit firing rates by 2.9 - 5.4 Hz when comparing two motor units at a time using the  
177 paired motor unit technique [5, 21-22]. The peak values observed in the current study were  
178 slightly higher than those observed experimentally for the lowest-threshold motoneurons at each  
179 force level, while the averaged values across all recruited motor units were a closer fit to the  
180 data. This is a reflection of inherent properties in the model built to describe the experimentally  
181 observed effect that PICs are recruited more readily in lower-threshold motoneurons [2,6].  
182 When assessing changes in motor unit coherence in the model after fitting to experimental firing  
183 rates in the FDI muscle, the results demonstrated that the removal of PICs had a modest effect  
184 on coherence, suggesting that PICs may not play a large role during isometric voluntary  
185 contraction in the FDI. The largest change in coherence was observed at 20% MVC, potentially  
186 due to an interaction between motor unit firing rates and the beta-modulated common input, as  
187 the mean firing rate at 20% MVC (17.6 Hz) is similar to the center frequency of the common  
188 input (17 Hz). Further simulations were performed to assess the effects of increased activation  
189 of PICs on motor unit coherence, represented by increased density of PIC-generating calcium  
190 channels on the dendrites. Although the ratio of common to independent input remained  
191 constant for increasing densities of PICs, motor unit coherence was observed to decrease in the  
192 presence of larger amplitude plateau potentials, particularly at the highest density level. These  
193 changes in coherence may be due to a dilution effect of the beta-modulated common input by  
194 PICs, as the amplitude of the synaptic input was increasingly reduced at higher density levels.  
195 The largest drop in coherence was observed at 20% MVC, as was the largest reduction in  
196 synaptic amplitude required to control for mean firing rate, supporting this hypothesis.  
197 Decreased coherence may also arise from a shunting effect of the PICs on other ionic  
198 conductances in the model, as PIC onset results in depolarization of the membrane potential,  
199 limiting the amount of current getting through from other sources [4]. Reduced coherence in the  
200 presence of PICs has been observed in a previous computational study [8], however only in the

201 case where beta-modulated oscillatory inputs comprised 90% of the total input signal. A later  
202 study assessing changes in corticomuscular coherence reported that removing PICs reduced  
203 coherence amplitude [14], however this was attributed to a higher ratio of independent to  
204 cortical input when controlling for firing rate. The current study investigates the effects of PICs  
205 on motor unit coherence in the presence of physiologically realistic branched and oscillatory  
206 common inputs, where the ratio between common and independent cortical inputs are held  
207 constant. The results of this study demonstrated that increasing the activation of PICs within  
208 motoneuron dendrites progressively reduced motor unit coherence, however only a modest  
209 effect was observed at levels consistent with experimental mean firing rates in the FDI muscle  
210 during isometric voluntary contraction.

211 **References**

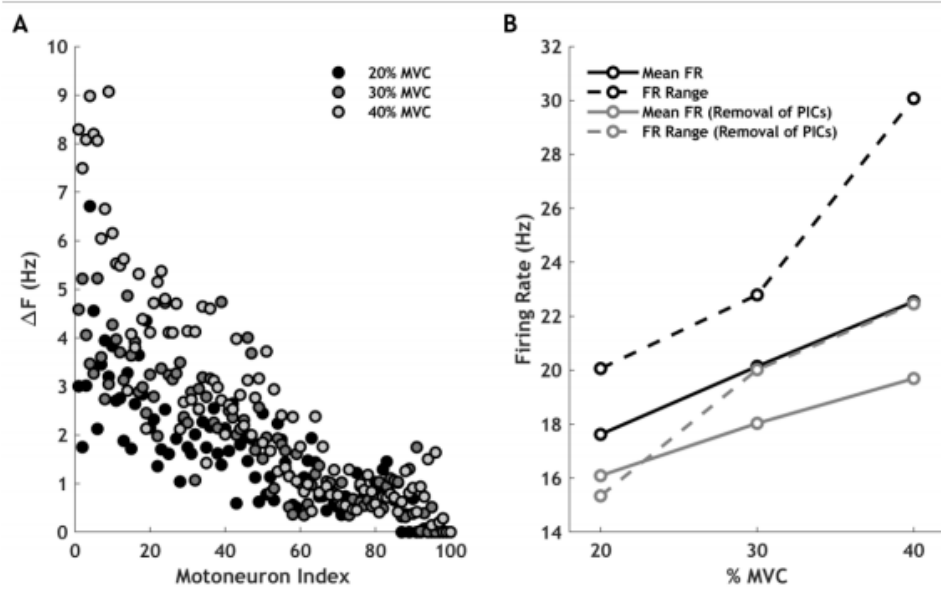
- 212 [1] C.J. Heckman, R.H. Lee, and R.M. Brownstone, Hyperexcitable dendrites in motoneurons  
213 and their neuromodulatory control during motor behavior, *Trends in Neurosci.*, vol. 26(12):  
214 688-695, 2003.
- 215 [2] C.J. Heckman, M.A. Gorassini, and D.J. Bennett, Persistent Inward Currents in Motoneuron  
216 Dendrites: Implications for Motor Output, *Muscle Nerve*, vol. 31: 135-156, 2005.
- 217 [3] R.K. Powers, S.M. Elbasiouny, W.Z. Rymer et al., Contribution of intrinsic properties and  
218 synaptic inputs to motoneuron discharge patterns: a simulation study, *J Neurophysiol.*, vol. 107:  
219 808-823, 2012.
- 220 [4] M.D. Johnson and C.J. Heckman, Gain control mechanisms in spinal motoneurons, *Front.*  
221 *Neural Circuits*, vol. 8(81): 1-7, 2014.
- 222 [5] M.D. Johnson, C.K. Thompson, V.M. Tysseling et al., The potential for understanding the  
223 synaptic organization of human motor commands via the firing patterns of motoneurons, *J.*  
224 *Neurophysiol.*, vol. 118: 520- 531, 2017.
- 225 [6] R.K. Powers and C.J. Heckman, Synaptic control of the shape of the motoneuron pool input-  
226 output function, *J Neurophysiol.*, vol. 117: 1171-1184, 2017.
- 227 [7] S.F. Farmer, F.D. Bremner, D.M. Halliday et al., The frequency content of common synaptic  
228 inputs to motoneurons studied during voluntary isometric contraction in man. *J Physiol*, vol.  
229 470: 127-155, 1993.
- 230 [8] A.M. Taylor and R.M. Enoka, Quantification of the Factors That Influence Discharge  
231 Correlation in Model Motor Neurons, *J. Neurophysiol.*, vol. 91: 796-814, 2004.
- 232 [9] L. McManus, X. Hu, W.Z. Rymer et al., Muscle fatigue increases beta-band coherence  
233 between the firing times of simultaneously active motor units in the first dorsal interosseous  
234 muscle, *J. Neurophysiol.*, vol. 115: 2830-2839, 2016.
- 235 [10] C.J. De Luca, R.S. LeFever, M.P. McCue et al., Control scheme governing concurrently  
236 active human motor units during voluntary contractions, *J. Physiol.*, vol. 329: 129-142, 1982.
- 237 [11] G. Kamen, S.S. Greenstein, C.J. De Luca, Lateral dominance and motor unit firing  
238 behavior. *Brain Res*, vol. 576: 165-167, 1992.
- 239 [12] G. Svirskis and J. Hounsgaard, Influence of membrane properties on spike synchronization  
240 in neurons: theory and experiments, *Network: Comp. in Neur. Sys.*, vol. 14(4): 747-763, 2002.
- 241 [13] S. Huh, R. Siripuram, R.H. Lee et al., PICs in motoneurons do not scale with the size of the  
242 animal: a possible mechanism for faster speed of muscle contraction in smaller species, *J.*  
243 *Neurophysiol.*, vol. 118(1): 93-102, 2017.
- 244 [14] E.R. Williams and S.N. Baker, Circuits Generating Corticomuscular Coherence  
245 Investigated Using a Biophysically Based Computational Model, *J. Neurophysiol.*, vol. 101: 31-  
246 41, 2009.
- 247 [15] M. Hines, A program for simulation of nerve equations with branching geometries, *Int. J.*  
248 *Biomed. Comput.*, vol. 24: 55-68, 1989.
- 249 [16] K. Seki and M. Narusawa, Firing rate modulation of human motor units in different  
250 muscles during isometric contraction with various forces, *Brain Research*, vol. 719: 1-7, 1996.
- 251 [17] C.J. De Luca and J.C. Kline, Influence of proprioceptive feedback on the firing rate and  
252 recruitment of motoneurons, *J. Neural Eng.*, vol. 9: (17pp), 2012.

- 253 [18] P.D. Cheney, E.E. Fetz, K. Mewes, Neural mechanisms underlying corticospinal and  
254 rubrospinal control of limb movements, *Prog. Brain Res.*, vol. 87: 213-252, 1991.
- 255 [19] D.M. Halliday, Generation and characterization of correlated spike trains, *Comp. in Biol.*  
256 *and Med.*, vol. 28: 143-152, 1998.
- 257 [20] M.M. Lowery and Z. Erim, A Simulation Study to Examine the Effect of Common  
258 Motoneuron Inputs on Correlated Patterns of Motor Unit Discharge, *J. Comp. Neurosc.*, vol. 19:  
259 107-124, 2005.
- 260 [21] E. Udina, J. D'Amico, A.J. Bergquist et al., Amphetamine Increases Persistent Inward  
261 Currents in Human Motoneurons Estimated From Paired Motor-Unit Activity, *J. Neurophysiol.*,  
262 vol. 103: 1295-1303, 2010.
- 263 [22] J.M. Wilson, C.K. Thompson, L.C. Miller, and C.J. Heckman, Intrinsic excitability of  
264 human motoneurons in biceps brachii versus triceps brachii, *J. Neurophysiol.*, vol. 113: 3692-  
265 3699, 2015.
- 266

267 **Figures**

268

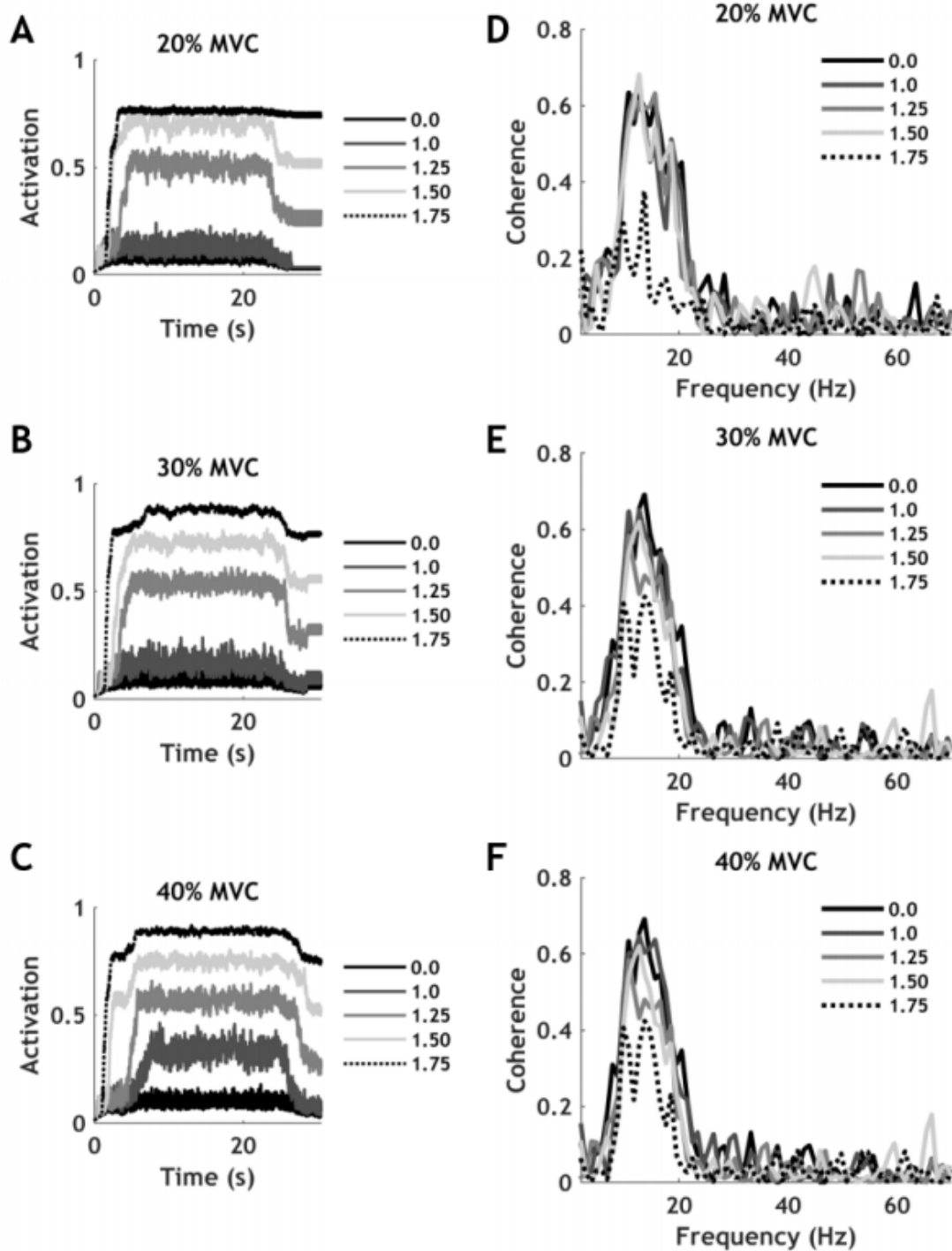
269 **Figure 1:** Mean firing rate (Mean FR) distribution at 20% MVC (A), 30% MVC (B), and 40%  
 270 MVC (C) in the model of the FDI muscle. The effect on the mean firing rate distribution after  
 271 removing PICs in the model is presented at each force level in gray.



272

273 **Figure 2:** Change in mean firing rate ( $\Delta F$ ) for each motoneuron within the pool when PICs are  
 274 removed from the model at each force level (A). Whole pool mean firing rate and mean firing  
 275 rate range at each force level both in the FDI model and when PICs are removed (B).

276



277

278 **Figure 3:** PIC plateau potentials averaged across all dendritic branches in the lowest-threshold  
 279 motoneuron of the pool at 20% MVC (A), 30% MVC (B), and 40% MVC (C). The  
 280 corresponding change in the coherence spectra is presented for increasing densities of calcium  
 281 channels on the dendrites (0, 1.0, 1.25, 1.50, and 1.75) at 20% MVC (D), 30% MVC (E), and  
 282 40% MVC (F).